LA-UR -83-1732

Conf-830874--9

Los Alamos National Laboratory is operated by the University of California for the United States Department of Energy under contract W-7405-ENG-36

LA-UR--83-1732

DE83 015239

TITLE PHOTOCONDUCTIVE POWER SWITCHES

AUTHOR(S) W. C. Nunnally and R. B. Hammond

SUBMITTED TO Proceedings of the Society of Photo-Optical Instrumentation Engineers Meeting, San Diego, CA, August 1983.

DISCLAIMER

Los Alamos Los Alamos National Laboratory
Los Alamos, New Mexico 87545

FORM NO 836 R4
ST NO 2629 5/81

MASTER

LA-UR-83-1732

Photoconductive Power Switches*

W. C. Nunnally, R. B. Hammond

Electronics Division, Los Alamos National Laboratory
Los Alamos, New Mexico 87545

Abstract

This paper outlines the advantages and the potential of photoconductive switches applied to high-power systems. The photoconductive effect can be used to switch large amounts of energy by changing the conductivity of a solid-state circuit element many orders of magnitude with a high-power laser. The simplicity of these devices offers many advantages in high-power applications when combined with high-power pulsed lasers. The surge capability, the switched energy gain, and the maximum average power for photoconductive power switches are discussed. In addition, the results of a 100-kV, 100-MW photoconductive switch experiment transferring 20 J in 200 ns are presented.

Introduction

The preliminary development and demonstration of scalable, photoconductive power switches (PCPSs) at Los Alamos[1-3] indicate that it is theoretically possible, in a single solid-state device, to switch high voltages (megavolts at 100 kV per centimeter length) and high currents (megamps at 10 kA per centimeter width) with more precision and higher efficiency than with any other technology. PCPSs operating at 135 kV (65 kV/cm) and 2 kA (4 kA/cm) have been experimentally demonstrated.[1] Because PCPSs can be designed to close faster with less inductance and less relative jitter than any other technology, power conditioning systems can be simpler, more efficient, and more compact. The large specific heat and the excellent thermal conductivity of photoconductive materials make the technology applicable to a large number of high-energy, high-average-power pulse applications.

Physical description

The basic PCPS geometry is illustrated in Fig. 1. Electrodes make contact at the ends of a photoconductive material such as silicon, GaAs, or InP. A PCPS does not have PN junctions because photoconductivity is a bulk phenomena, and thus, a single device can be scaled to any voltage or current requirement. The length ℓ of the photoconductive material block is determined by the desired operating voltage; the width w is determined by the desired operating current or desired inductance; and the effective optical absorption depth d_e is determined by the type of photoconductive material and by the optical control wavelength.

This arrangement differs from the light-activated silicon switch (LASS)[4] in two aspects. First, the LASS device uses the four-layer, silicon-controlled rectifier (SCR) structure with three series PN junctions, one of which must hold-off the applied voltage before switching, while the photoconductive power switch distributes the applied voltage across the entire length of the photoconductive material between the electrodes. Second, the region between the electrodes is uniformly illuminated in the PCPS to change the conductivity of the entire device simultaneously, while the LASS device uses the photoconductive effect to change only the conductivity of the gate region of the SCR structure.

Operation

Optical control

The conductivity of a PCPS can be controlled with electrons, ions, or photons. For the purpose of this discussion, only photon sources will be considered. Optical control has the inherent advantage of isolation for any high-voltage switch. For a PCPS, optical control has the further advantage of very fast closure of the switch because of the large amount of optical energy that can be delivered in a very small period of time in a high-power laser pulse. In addition, the optical energy can be distributed in space with very precise time resolution to control one large switch or many separate switches either simultaneously or in a precise sequence determined by the transit-time differences of the controlling optical path lengths.

* This work is sponsored by the Los Alamos National Laboratory Engineering Sciences Directorate and the Department of Energy.

Bulk carrier generation

A photon with an energy greater than the photoconductor band gap produces an electron-hole pair in the photoconductive volume. When uniformly illuminated, the conductivity of the entire switch can be changed in the time in which the optical energy is delivered. The bulk generation of electron-hole pairs in the conduction volume removes the device speed transit-time limitation present in other switching technologies. Thus, device speed is decoupled from device size or power. As illustrated in Fig. 2, a PCPS can be closed in a time scale not possible with other technologies. The change in resistance or closure of a conventional switch is initiated at a single point between the electrodes. Avalanche processes must then generate additional carriers. However, as the carrier density increases, the electric field in the switch decreases, reducing the carrier generation rate. Thus, conventional high-power switches have a decaying exponential resistance during turn-on. In contrast, the resistance of the PCPS is determined by an external optical source with closure time determined by the optical power.

Carrier removal

The carriers generated with the input optical energy are removed from the conduction process in two ways. First, the carriers recombine within the photoconductive material in a time usually determined by the trap doping level. For very high-speed photoconductive detectors, the recombination time is chosen to give the fastest possible falltime. As shown in Fig. 3, heavy doping produces recombination times less than 100 ps. For a closing switch, long recombination times are desired so that conduction will persist after the end of the optical pulse. Recombination times of 20 μs have been measured at Los Alamos in intrinsic (pure) single-crystal silicon so that electrical pulses with durations less than 1 μs can be switched with a much shorter optical pulse. The conductivity in the switch can be maintained by supplying additional optical energy during conduction.

Carriers are also removed from the conducting volume at the contacts. If the junction between the metal and the conductor forms a Schottky barrier, only a fraction of the carriers will be reinjected. To maintain high conductivity, the contacts must be ohmic in nature without a Schottky barrier.

Limitations

The operating voltage of a PCPS is limited by the electric breakdown strength of the photoconductor or of its surface. The bulk electric field strength of most semiconductors is about 100 kV/cm, and initial experiments at Los Alamos have operated at up to 65 kV/cm, and improvements are being developed.

To avoid thermal runaway in a silicon PCPS, the carrier density must remain below 10^{18} cm^{-3}. This translates into a current density of less than 100 kA/cm^2 or a line current density of 10 kA/cm with an optical absorption depth of 1 mm. Experiments at Los Alamos have demonstrated a line current density of 4 kA/cm.

The electrical pulse length and the pulse repetition rate are limited by the average power obtainable with present laser systems. However, many low-pulse-rate applications with electrical pulses less than 1 μs are possible with present-day lasers.

Additional advantages

Circuit-independent control

The conductivity of a PCPS is controlled by the external optical source and not by the circuit to which it is connected. Thus, a PCPS designed to operate at 10 kV should close in a similar manner at 10 V. This advantage reduces the effects of voltage variations and transients.

Inductance-resistance ratio

Because the inductance of a PCPS is proportional to its width and the resistance is independent of width, the ratio of switch inductance to resistance can be designed for a specific application by varying the switch width.

Thermal management

For fixed total optical input, the total resistance is independent of width. Electrical energy dissipated per unit volume in the switch is reduced by increasing the switch width. The area available for heat removal also scales as the device width so that the maximum average power of operation scales as the switch width. The thermal energy deposited in the switch must be transported only the effective optical absorption length to the large surface area and must be removed from the conducting medium.

Implementation of alternate circuit concepts

The fast closure, precise control, optical isolation, and low inductance possible with PCPSs make the implementation of standard circuits more efficient and the application of

alternate concepts feasible. For example, the switching of a Blumlein line[5] pulse generator with a high-efficiency, very low-inductance PCPS is illustrated in Fig. 4. The use of the PCPS with the Blumlein line will provide a faster output pulse risetime and reduce the percentage of stored energy deposited in the switch compared with that of conventional technology, especially in very low-impedance systems. The control of a single Blumlein line can be extended to the stacked line[6] concepts illustrated in Fig. 5.

Analysis

Photoconductive switch resistance

The resistance R_s of the photoconductive volume of Fig. 1 is given by[3]

$$R_s = \ell^2 E_\lambda / [e\mu E_L (1 - r)] \quad , \tag{1}$$

where e is the electron charge, μ is the sum of the carrier mobilities, E_L is the optical energy, r is the material reflectivity, and E_λ is the photon energy. Note that the photoconductive resistance is independent of width for constant optical energy deposited in the photoconductive volume.

Adiabatic characteristics (I^2t)

The amount of energy that can be absorbed by a switch is determined by the I^2t product. The value of the I^2t product for a photoconductive power switch when an infinite recombination time

$$(I^2t)_c = \rho w d_e c_p \Delta T e\mu(1 - r)E_L/(E_\lambda \ell) \quad , \tag{2}$$

where c_p is the material specific heat, ρ is the material density, and ΔT is the change in device temperature during conduction. Note that junction devices are limited to a maximum temperature of 180°C, but PCPSs can operate with much higher ΔT values. As an example, for E_L = 10 J, w = 1 m, ℓ = 0.1 m, ΔT = 1000°C, r = 0.3, $c_p = 0.7 \times 10^3$ J/kg-°C, $\rho = 2.33 \times 10^3$ kg/m^3, μ = 0.13 m^2/s, and $E_\lambda = 1.2 \times 10^{-19}$ J for 1.06-μm wavelength illumination, $I^2t = 1.5 \times 10^7$ A^{2}s. Thus, this switch will conduct a current of 10 MA for time t_{ep} = 150 ns with an optical trigger energy of 10 J.

Switched energy gain

The switched energy gain of a photoconductive switch is best described as the ratio of the energy E_{load} transferred to the load to the laser energy E_L incident on the surface. If a matched system is considered where the source impedance is equal to the load impedance and the switch resistance is much lower than the load impedance, then the energy delivered to the load (assuming that the electrical pulse risetime is much less than the pulse length) is

$$E_{load}/E_L = \rho w d_e Z_L E_{max} c_p \Delta T e\mu(1 - r)/(V_s E_\lambda) \quad , \tag{3}$$

where the switch length is the ratio of the source voltage V_s to the maximum electric field E_{max} and Z_L is the load impedance. The switched energy gain is limited by the amount of heat that the switch can absorb before damage occurs.

Maximum average power

The maximum average power delivered to a load through the switch is related to the maximum average power that can be removed from the switch volume at a temperature consistent with switch operation. The average power delivered to the load in a repetitively pulsed system is

$$P_{avg} = I^2 R_L t_{ep} PRR = h(T_{edge} - T_{fluid}) \gamma w \ell / \delta \quad , \tag{4}$$

where I is the current through the switch, R_L is the load resistance, t_{ep} is the electrical pulse length, PRR is the pulse repetition rate, h is the heat transfer coefficient between the switch and the cooling fluid, γ is some multiple of the switch frontal area available for cooling, w is the switch width, ℓ is the switch length, δ is the ratio of the switch resistance to the load resistance, and T_{edge} and T_{fluid} are the temperatures of the switch body and the cooling fluid, respectively. If h = 1000 J/s, R_s = 0.01 R_L, δ = 0.01, ($T_{edge} - T_{fluid}$) = 100°C, ℓ = 0.1 m, w = 1 m, γ = 10 m^2°C, I = 50 kA, t_{ep} = 100 ns, and PRR = 10 kHz, then the peak power delivered to the load is 10 GW, and the average power delivered to the load is 10 kW. The average power that must be removed from the switch in this example is equal to γP_{avg} or 100 kW.

Preliminary high voltage experimental results

Device design and fabrication

A series of experiments were performed on bulk silicon photoconductors using a Q-switched Nd:glass laser as the excitation source. This source provided a long absorption

length (1 mm) and a large excess in pulse energy. The silicon devices were fabricated from 1000 Ω-cm, n-type silicon. Samples were cut 2.5- x 0.5- x 0.5-cm^3. The saw-cut samples were lapped on all surfaces to 5-μm grit-size alumina. The four longitudinal corners were smoothed to prevent local electric field enhancement; following this, the samples were etched in CP4 at 0°C. At this point, some samples were oxidized in an O_2 ambient at 1100°C for 4 hours. For the oxidized samples, the oxide on the ends of the parallelepiped was removed with HF; sometimes these ends were lapped. Finally, evaporated aluminum contacts were deposited on the sample ends, which were then sintered at 500°C for 2 minutes.

Experimental arrangement

The test circuit for high-voltage, high-current photoconductive switch experiments is shown in Fig. 6. The silicon bar used for switch evaluation was placed between two brass electrodes, and electrical contact was made with a spring arrangement that compressed the sample with approximately 10-kg force. One of the electrodes was grounded through a very low-inductance current-viewing resistor with a bandwidth of approximately 2 GHz. The other electrode was connected to two parallel 50-Ω RG-19 coaxial cables 18.5 m in length through a load resistor tube filled with copper sulfate. The conductivity of the load resistor solution was selected to match the impedance (25 Ω) of the two coaxial cables. The two parallel cables were pulse-charged to between 100 and 300 kV in approximately 1.5 μs upon triggering the Marx circuit. The entire high-voltage test assembly at the end of the coaxial cables was immersed in several dielectric fluids, including water and ethylene glycol, to prevent high-voltage arcs between points in the circuit. The water dielectric was circulated through an ion exchange column and filtered to increase the resistivity, and air bubbles were removed to prevent inadvertent discharge.

The light source that caused conduction in the silicon sample consisted of a Q-switched Nd:glass laser that could deliver up to 3 J of optical energy in a 20-ns full-width at half maximum (FWHM) laser pulse. The laser energy in the 20-ns pulse was varied from 0.03 to 3 J, and two cylindrical lenses were used to provide a rectangular beam pattern that distributed the optical energy in a relatively uniform manner over the surface area of one side of the silicon bar from electrode to electrode. In addition, a dielectric tube terminated with a quartz flat was inserted into the liquid-insulated, high-voltage region to transport the optical energy most of the distance through the liquid without attenuation or distortion. The high-voltage or high electric field stress on the sample required that the ends of the silicon bar samples be recessed in brass electrodes so that the simple contacts discussed would not produce free electrons at surface irregularities. Both electrodes were grooved to permit optical energy to cover the entire sample, even into the recessed region on one side, so that the entire device could be activated but still have the sample contacts in the low-field region. Contact between the aluminum-coated silicon and the brass electrodes was aided by a heavy coating of indium solder on the electrodes.

The current through the switch was measured with a low-inductance current-viewing resistor in the ground electrode. The voltage on the source cables during pulse charge and photoconductive discharge was measured with a capacitance-compensated voltage divider (Fig. 6). The optical pulse shape was determined using a small photoconductive detector, and the pulse energy was determined with a thermocouple.

The silicon samples were placed between the electrodes, and the pulse voltage was applied several times before applying the optical pulse. Without the optical pulse, the devices remained an open circuit unless the applied voltage exceeded the surface flashover electric field. When the optical pulse was applied to the silicon surface, the switch closed and current was observed in the load resistor and through the switch.

Experimental results

In these initial experiments, several samples were evaluated in the high-voltage circuit. The source voltage and the switch current for a single-pulse operation at approximately 100 kV is shown in Fig. 7. The electrical pulse length is determined by the the two-way transit time (200 ns) of the coaxial cables, and the peak current is determined by the ratio of the source voltage to the sum of the cable impedance and the load resistance, or approximately 1.8 kA. The peak electrical power in the load for the result in Fig. 7 is approximately 80 MW, with a total energy transfer of about 15 J. The peak current of 1.8 kA for a 0.5 cm width scales to about 360 kA/m, and the electric-field stress on the sample is approximately 40 kV/cm. The electric field stress was limited to 40 kV/cm by surface flashover in the water environment in much less than the 100 kV/cm expected in a dry environment.

Several important observations can be made from the experimental results. The current decay after the laser pulse terminated (Fig. 7) probably results from the contact injection inefficiency of the sample or from space charge. The transit time of the device is

approximately 200 ns so that an appreciable number of the carriers generated by the 20-ns laser pulse are swept out of the switch region during the electrical pulse. The inefficient contacts are probably not injecting new carriers. The switch resistance increases to a level comparable with the load and source resistances, thus, decreasing the circuit current. This also causes a mismatch of the transmission line source and leads to reflections. The current risetime is ~5 ns, which may be determined by the laser pulse power. The circuit-limited risetime is ~0.5 ns, and the current probe risetime is < 1 ns.

The current excellent capability of the switch was obvious when one observed the extensive damage that occurred when the sample surface tracked. The surface flashover when the cables were charged resulted in a very high-current-density arc channel along the sample surface that melted a 0.5-mm-deep groove in the surface. The discharge of the energy stored in the cables in a surface flashover also resulted in a large shock wave transient that fractured the silicon sample. However, the photoconductive device was very rugged when operated properly. Conducting the large current did not affect subsequent operation of the sample. Current in the sample was evidently uniformly distributed across the sample width so that the current density was much lower than in the surface arc case. One sample that was fractured perpendicular to the current path by a surface discharge remained between the electrodes and continued to function as a switch without voltage and current response degradation. The current flowing in the silicon was observed to arc across the fracture in a uniform current sheet.

Conclusions

Photoconductive power switches have the potential to close faster (and, thus, more efficiently) with more precision, less relative jitter, and with less inductance than any other technology. They also offer the standard advantages of optical control isolation. The bulk nature of the photoconductive phenomena will permit the design of a single solid-state switch for any voltage or current or of multiple photoconductive switches to be closed in a precise sequence. The thermal characteristics of photoconductive materials and a geometry that promotes heat removal permit very large surge capabilities and high average-power operation. These characteristics and initial experiments indicate that photoconductive switch technology has the potential to be the control technology for future high-power applications.

References

1. W. C. Nunnally and R. B. Hammond, "Photoconductive Power Switches," Los Alamos National Laboratory, LA-9759-MS (April 1983).

2. W. C. Nunnally and R. B. Hammond, "Optoelectonic Switch for Pulsed Power," in Picosecond Optoelectronic Devices, C. H. Lee, Ed. (Academic Press, New York, 1983).

3. W. C. Nunnally, "Accelerator Applications of Photoconductive Power Switches," Los Alamos National Laboratory, LA-9760-MS (April 1983).

4. O. F. Zucker, J. R. Long, V. L. Smith, D. J. Page, and J. S. Roberts, "Nanosecond Switching of High Power Laser Activated Silicon Switches," UCRL-77649 (November 1975).

5. A. D. Blumlein, US Patent No. 589127 (October 1941).

6. R. A. Fitch and V. T. S. Howell, "Novel Principle of High Voltage Generation," Proceedings of the IEEE, Vol. 111, No. 4 (April 1964).

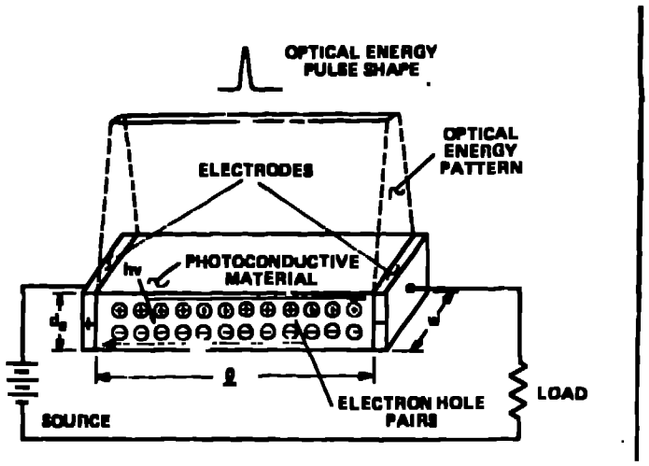

Fig. 1. Photoconductive power switch geometry.

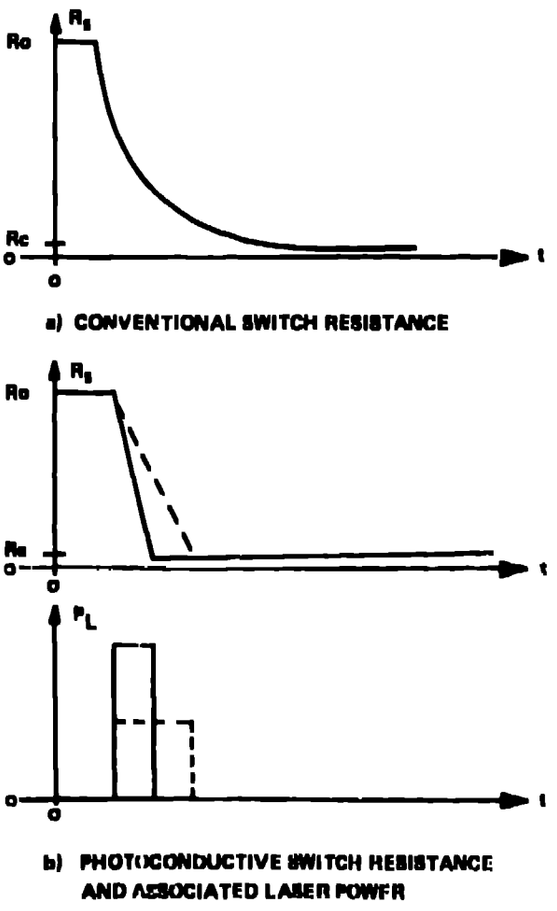

Fig. 2. Comparison of conventional and photoconductive switch closures.

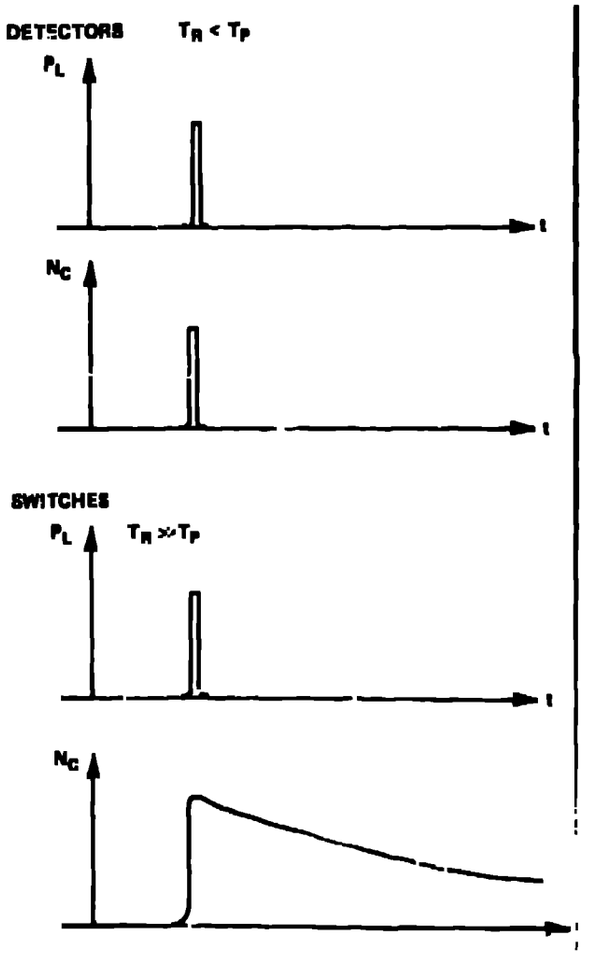

Fig. 3. Photoconductor recombination times for detectors and switches.

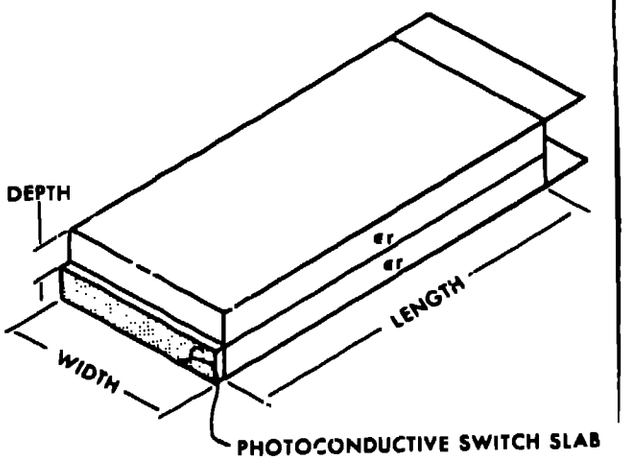

Fig. 4. Photoconductively switched Blumlein line pulse generator.

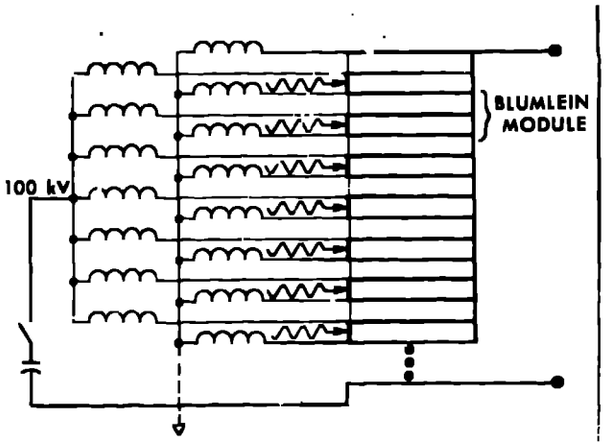

Fig. 5. Photoconductively switched stacked line module.

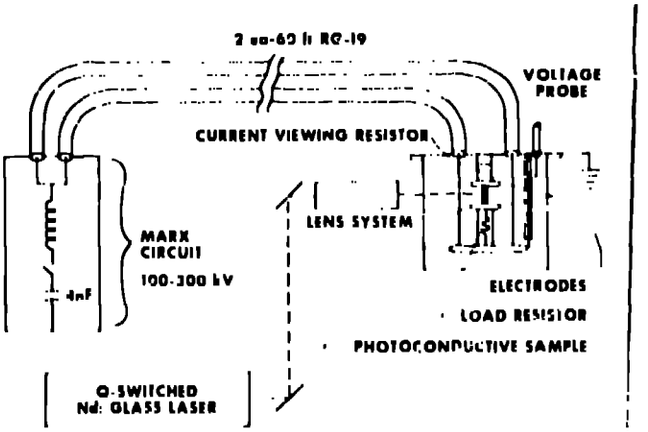

Fig. 6. Experimental arrangement for photoconductive pulse power switch.

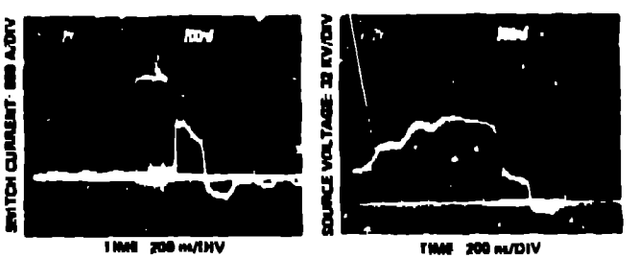

Fig. 7. Photoconductive pulse power switch experimental results.